ACS OMEGA

Open Access

http://pubs.acs.org/journal/acsodf

Article

How the Orientation of BN Units Influences the Aromaticity of Some *Iminobora*-Benzenes

Luz Diego,* David Arias-Olivares, Diego V. Moreno, Erick Cerpa, and Rafael Islas*

Cite This: *ACS Omega* 2025, 10, 5900−5908

Read Online

ACCESS | Metrics & More | Article Recommendations | Supporting Information

ABSTRACT: In the current work, the impact of the orientation of the BN units in some proposed isomers of *iminobora*-benzene ($B_6C_6N_6H_6$) is analyzed. The analysis is oriented toward determining whether the orientation plays an important role in electronic delocalization (aromaticity). The alternation of the BN units generates several isomers, which were built arbitrarily and systematically with the main goal of measuring their respective electronic delocalization. For the analysis of aromaticity, multiple methodologies (AdNDP, AV1245, AVmin, ELF, LOL, MICD, and $\mathbf{B}^{ind}$) were employed, all of which produced consistent trends. Moreover, the alternation of the BN units affects not only electronic delocalization but also relative stability, with relative energy values of up to 85 kcal/mol observed among the isomers. Interestingly, the most aromatic isomer is the least stable isomer, while the most stable isomer is, with some methodologies, the least aromatic.

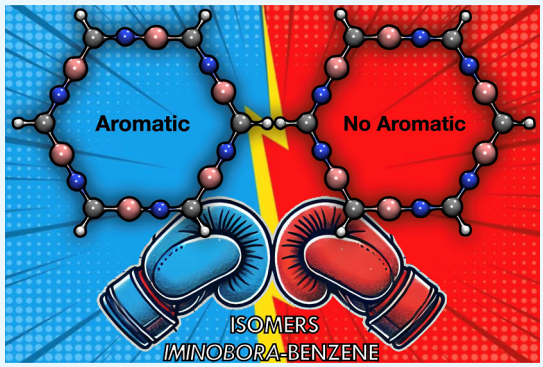

1. INTRODUCTION

Carbomers are defined by Chauvin as extended molecules, which are obtained by the inclusion of C≡C (or C_2) unit in each bond of any other molecule.[1−3] The simplest example is acetylene, which could be considered as the carbomer of molecular hydrogen. For cycles, the inclusion of C_2 units generated larger cycles. For example, the carbomer of benzene (C_6H_6, D_{6h}) is named *carbo*-benzene ($C_{18}H_6$, D_{6h}), and both molecules preserve the symmetry and some characteristics, such as electronic delocalization. The same procedure could be applied to borazine (B_3N_3H, D_{3h}) and, after the inclusion of six C_2 units, the ring *carbo*-borazine ($B_3C_{12}N_3H$, D_{3h}) is obtained. In a work published in 2014, Jalife et al. replaced the C_2 units of the *carbo*-borazine by *iminobora* (BN) units, both chemical entities with eight valence electrons, and proposed a new inorganic compound, which was labeled as *iminobora*-borazine.[4] Finally, the aromaticity of *carbo*-benzene, *carbo*-borazine, and *iminobora*-borazine was analyzed, and it was observed that the electronegativity difference between boron and nitrogen affected the electronic delocalization.[4] In this line, the *carbo*-aromaticity[5] of other systems, such as *carbo*-cages[6] or *carbo*-metallabenzenes[7] was studied. The inclusion of BN units in carbon rings is not a new target in computational chemistry. For example, the structural changes and electronic effects following the isoelectronic monosubstitution of carbon atoms with B and N atoms have been studied in cyclo[18]carbon (a large carbon ring).[8] Cheng et al. reported that when analyzing the BNC_{16} isomers, the most stable isomer is the least aromatic species. To the best of our knowledge, the systems described above contain B, C, and N atoms, where aromaticity is not related to stability.[8] Additionally, azaborine rings have been studied. In particular, Baranac-Stojanovic reported the aromatic behavior of 1,2-, 1,3-, and 1,4-azaborines, concluding that the most aromatic isomer is also the least stable one.[9] In 2015, Srivastava and Misra proposed carborazine, an isoelectronic analogue to benzene. Carborazine is generated by substituting three adjacent carbon atoms (CCC) with BCN units, resulting in the chemical formula $B_2C_2N_2H$. These compounds are slightly more aromatic than borazine.[10] Years later, in 2020, Anstöter, Gibson, and Fowler modeled the aromatization of $(BN)_nH_n$ azabora-annulenes. In particular, they found that "borazocine", $[B_4N_4H_8]^{2-}$, has a diatropic character (comparable with benzene), and it could form coordinated compounds such as sandwich complexes.[11] An analysis of the nature of the chemical bond in borazine was conducted by Kalemos. In that work, the authors analyzed the excited states of the BH and NH fragments to form the ground state of borazine. The author also analyzed boraxine and carborazine using the same methodology.[12] Wu et al. established that the aromaticity difference between $B_6C_6N_6$ and B_9N_9, isoelectronic species of cyclo[18]carbon (C_{18}), is due to the insertion of C atoms in $B_6C_6N_6$ showing a slight negative charge in C atoms, which regulates the electronic structure of the ring. Comparing $B_6C_6N_6$ with two other

Received: October 26, 2024
Revised: January 27, 2025
Accepted: January 31, 2025
Published: February 7, 2025

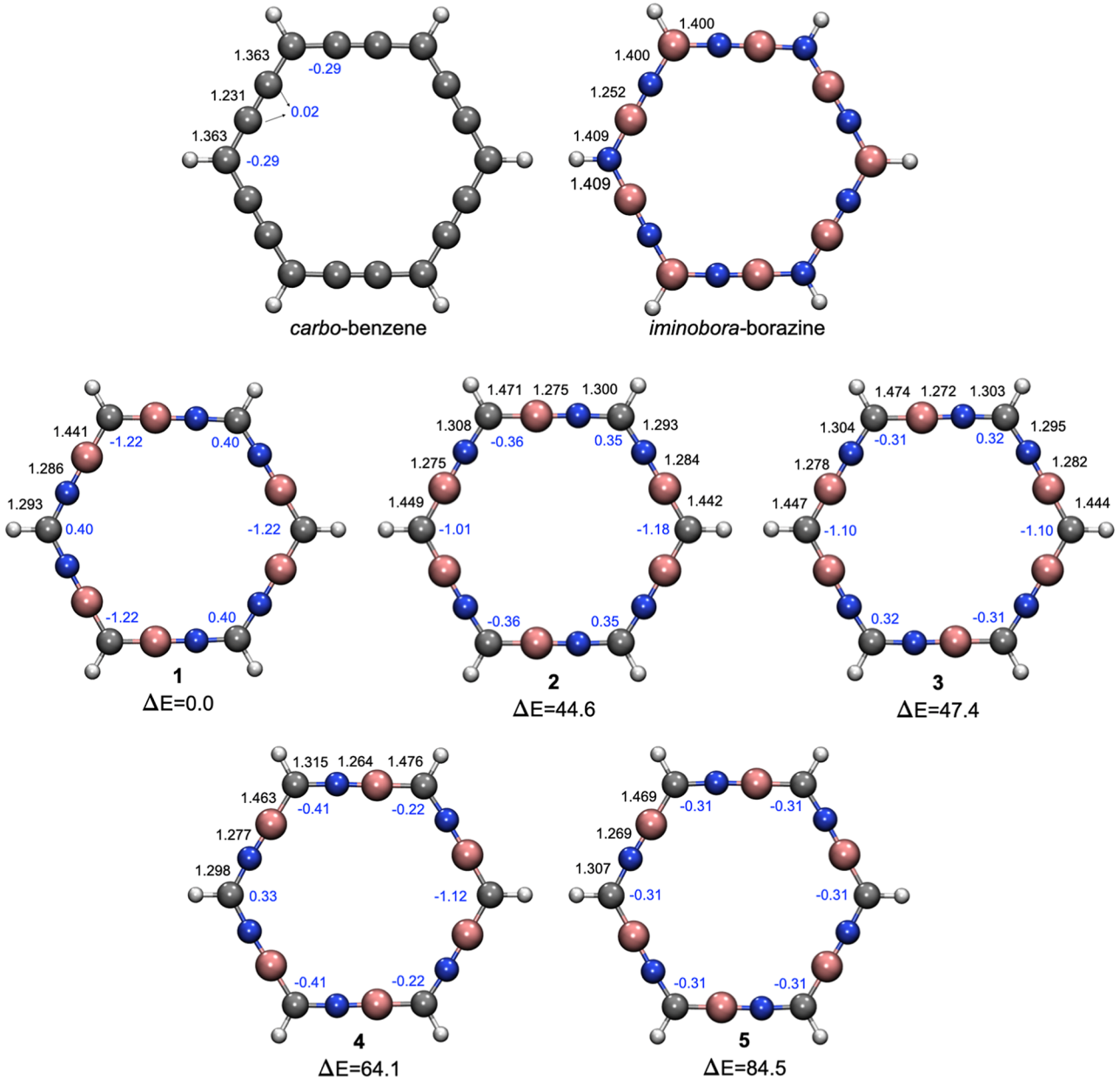

Figure 1. Black numbers represent the bond lengths of the isomers proposed for *iminobora*-benzene, and they are expressed in Å. Blue numbers represent the natural charges of the carbon atoms, and they are in lel. Blue, pink, dark-gray, and white spheres represent nitrogen, boron, carbon, and hydrogen atoms, respectively. Relative energies are expressed in kcal/mol.

isomers, which do not have an alternating structure of B, C, and N, their relative energies of the isomers are lower by 280.0 and 250.2 kcal/mol.[13] The authors reported that $B_6C_6N_6$ is aromatic while the other two isomers present nonaromaticity like B_9N_9. Also, they provided a conclusion that the $B_6C_6N_6$ molecule has a double aromaticity similar to that of C_{18},[13] a concept provided by Fowler[14] for all-carbon rings and previously used by Chandrasekhar, Jemmis, and Schleyer[15] for the molecule 3, 5-dehydrophenyl cation ($C_6H_3^+$).

This interest in boron−nitrogen isoelectronic molecules related to aromatic carbon rings originated with Stock and Pohland's discovery of borazine in 1926[16] and its subsequent comparison with benzene, which led Wiberg to label borazine with the pseudonym of "inorganic benzene" due to its 6 π-electrons and hexagonal planar geometry (D_{3h}).[17] The reactivity of borazine differs from that observed in benzene. Borazine prefers addition reactions over substitution reactions, although Chiavarino reported electrophilic reactions.[18,19] Borazine is classified as a weak π-aromatic compound,[20] and the inclusion of a metallic center in borazine, following the isolobal analogy,[21] has created rings named metallaborazines, in which the low-aromatic character is not affected by the inclusion of metallic centers.[22] Energy-based calculations determine that borazine exhibits 50% of the aromatic character of benzene.[23] However, the current consensus is that borazine is weakly aromatic, which has been experimentally supported by charge density analysis conducted by Merino-García et al. in 2022.[24]

In the current work, some isostructural isomers of *iminobora*-benzene were analyzed with the goal of measuring the impact of the orientation of the BN units on their electronic delocalization. It is known that the electronegativity

https://doi.org/10.1021/acsomega.4c09769
ACS Omega 2025, 10, 5900−5908

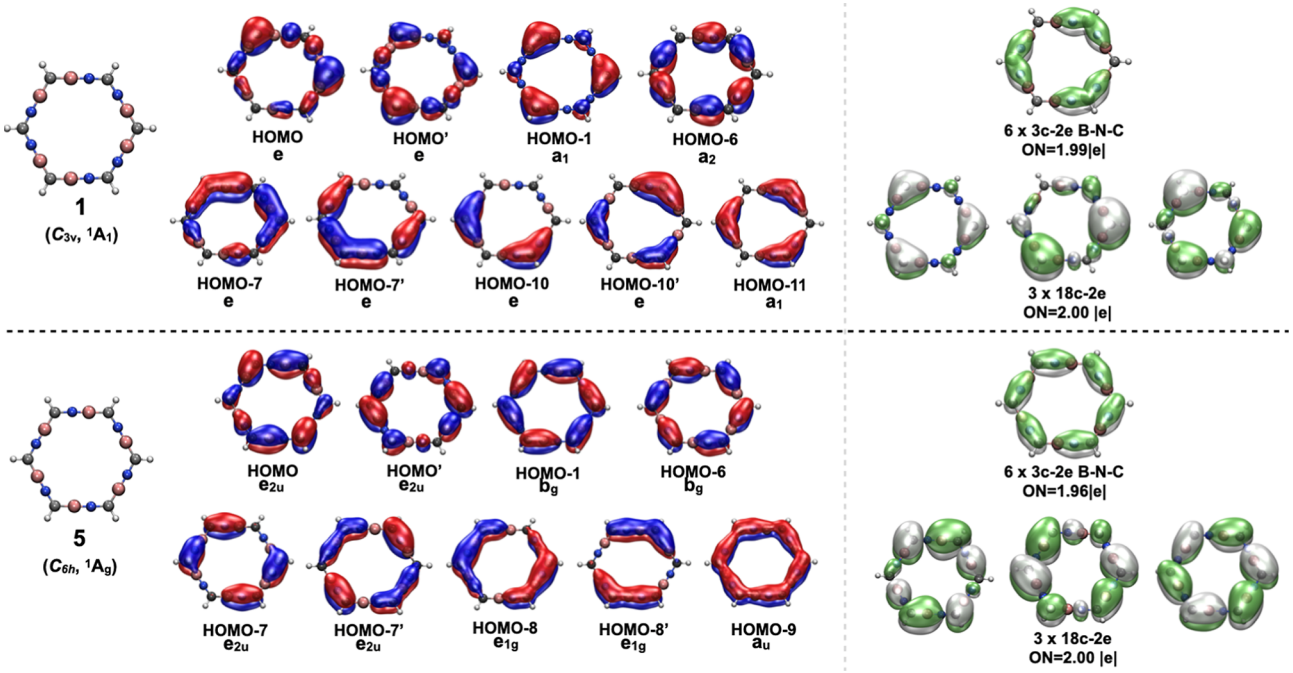

Figure 2. Canonical molecular orbitals of the 18 π electrons (CMOs) on the left and the AdNDP bond pattern on the right for the π-bonds on the z-axis of isomers **1** and **5** at PBE0-D3/def2-TZVP level.

difference between nitrogen and boron atoms plays a significative role in the electronic delocalization of borazine.[20]

2. COMPUTATIONAL DETAILS

The isomers were designed arbitrarily, proposing the orientation of the BN units. Several isomers were initially proposed, but some of them turned out to be the same molecule. Therefore, only five unique isomers were studied, and their geometries were optimized and characterized considering the functional PBE0[25−27] and the def2-TZVP[28] basis set employing the Gaussian 16 software.[29] The stability of the wave function was confirmed through the algorithm[30,31] included in Gaussian 16. Topological analysis over all critical points was done with the same level of theory by means of the AIMALL package 19.19.12.[32] Natural charge analysis was performed in terms of natural population analysis (NPA)[33] using the NBO 6.0 program.[34] Adaptive natural density partitioning (AdNDP), developed by Zubarev and Boldyrev,[35,36] was used to recover the Lewis electron pair concept, locating 2-electron bonds with n centers (nc-2e) through Multiwfn program,[37] where the molecular structure and orbitals were visualized using VMD 1.9.3.[38] Also, with the Multiwfn program, AV1245[39] and AVmin[40] were calculated at the PBE0/def2-TZVP level of theory, considering Grimme dispersion. For electronic localization function (ELF) and localized orbital locator (LOL), the wave functions employed were computed at PBE0/def2-TZVP generated by Gaussian 16. Maps of the ELF were plotted directly with the Multiwfn program, and the isosurfaces of LOL-π were made with the VMD 1.9.3 program employing the cube files generated by Multiwfn. The magnetically induced current density (MICD) was calculated using the linear response function[41] and the perturbing operator for the magnetic field. The MICD was plotted in the streamline representation of the current density using PyNGL[42] and computed via DIRAC 17[43] at the DFT level of theory with the PBE0 functional. The four-component Dirac−Coulomb Hamiltonian was used alongside the unrestricted kinetic balance.[43] The cc-pVDZ basis set was employed for all atoms.[44] Furthermore, the MICD was integrated through the two-dimensional Gauss−Lobatto quadrature in a 2D plane (XY) extended from the molecular center to $15a_0$. The integration is plane-dependent; therefore, other 2 planes were selected (±120°), bisecting the triple bond. The shielding tensors employed for the calculation of the induced magnetic field, i.e., $\mathbf{B}^{ind}$,[45] were computed with the PBE0/def2-TZVP level in Gaussian 16. The z-component of the $\mathbf{B}^{ind}$, called B_z^{ind} (which is equivalent to $NICS_{zz}$[46]), was reported in the current work.

3. RESULTS AND DISCUSSION

3.1. Structural Analysis. The optimized geometries are depicted in Figure 1 and are ordered by their relative energies, with the most stable isomer labeled as **1** and the least stable as **5**. This last isomer was previously reported by Soncini et al., who concluded that the isomer exhibited aromatic character.[47] There is no significant difference in the bond lengths of the isomers; therefore, the alteration in the orientation of the BN units does not impact their structures. Furthermore, QTAIM shows that all bond critical points (BCP) exist between CN, CB, and BN units. While all of them are symmetrical in the *carbomer* system, the displacement of BCP follows the atomic radii pattern, i.e., the BCP is closer to C in CN units, closer to B in CB units, and closer to B in BN units. This does not provide meaningful insight into its structural stability or any relation to their relative energy and aromatic character. Additionally, the ring critical point (RCP) is also analyzed, and all the parameters remain virtually the same among all systems, including the stress tensor and its eigenvalues. Only two parameters show a significant change: (i) the RCP changes its position. While the carbomer's RCP is located at (0,0,0), **5** is slightly deviated from this position, followed by **3** and **1**. The highest displacements belong to **2** (0.1 Å) and **5** (0.2 Å) along

https://doi.org/10.1021/acsomega.4c09769
ACS Omega 2025, 10, 5900−5908

the z-axis. (ii) The RCP electrostatic potential (ESP, see Table S1 from ESI) shows a positive correlation between the isomer's relative energy and its ESP value. Thus, the ratio between the most stable isomer **1** (ESP = −0.0123 au) and the least stable isomer **5** (ESP = −0.0092 au) is 1.34. This positive correlation could be related to the relative energy stability and its aromaticity (vide infra).

In Figure 1, the natural charges of the carbon atoms are presented, with the electronegativity of the nearest-neighbor carbon atoms playing a significant role. In the case of NCN bonds, the higher electronegativity of the nitrogen atoms induces a positive charge on the carbon atom. However, in the other two cases (NCB and BCB), the charges on the carbon atoms remain negative. Consequently, **1** has three carbon atoms with positive charges, while **5** has all its carbon atoms with negative charges. This difference in charge distribution could be related to the stability based on relative energy, where all negatively charged carbon atoms are found in the less stable **5** (84.5 kcal/mol) in comparison to **1**.

Analysis of the molecular orbitals revealed that all of the isoelectronic structures contain 78 electrons distributed in 39 canonical molecular orbitals (CMOs). Of these, 18 π-electrons occupy 9 of the π-CMOs, which are delocalized along the ring (see Figures S1−S5 from ESI). Figure 2 shows the π-CMO values of **1** and **5**. In particular, **5** is notable for its uniform delocalization with a homogeneous π-CMO (HOMO−9), which extends over the peripheral atoms of the ring; a similar pattern is observed in *carbo*-benzene (see HOMO−9 in Figure S6 from ESI). In contrast, **1** shows an π-CMO (HOMO−11) composed of three delocalized π orbitals, but they are "interrupted" by three carbon atoms that do not participate in the total ring delocalization. Similar behavior was observed in *iminobora*-borazine, where the delocalization is interrupted by three boron atoms (see HOMO−11 in Figure S7 from ESI). On the other hand, AdNDP analysis shows that (i) all systems form 2c−2e σ-bonds at the perimeter of the ring and (ii) present six in-plane 2c−2e π-bonds, originated from the lateral overlap of the p-orbitals in the B and N atoms (see Figures S8−S12 from ESI). However, each structure is distinguished by the presence of nine π-bonds perpendicularly delocalized with respect to the plane, which are distributed into six 3c−2e bonds and three 18c−2e bonds. Although the vast majority of structures tend to form 3c−2e BNC overlapping π-bonds that connect at the C atom, Figure 2 shows the AdNDP bonding scheme for **1** and **5**, highlighting the following: (i) in **1**, the largest number of 3c−2e BNC overlapping π-bonds with a high occupancy number (ON) were identified, similar to *iminobora*-borazine, although with the difference that the overlapping bonds are connected to the B atoms (see Figure S13 from ESI); and (ii) in **5**, no overlapping bonds are formed, but a continuous and uniform distribution of the six 3c−2e BNC π-bonds and the three 18c−2e π-bonds that are delocalized along the entire ring, similar to *carbo*-benzene, is observed (see Figure S14 from ESI).

Although, the AdNDP analysis indicates that all structures comply with Hückel's rule ($4n$ + 2 π-electrons), which is consistent with CMO analysis, it is important to highlight that the distribution of π-bonds, closely related to the alternating orientation of the BN units, qualitatively suggests a higher aromatic character in **5**.

3.2. Aromaticity. The ELF[48,49] and LOL[50] are functions used to illustrate the degree of electron delocalization in chemical systems, facilitating covalent bonding analysis by revealing regions of molecular space where the probability of finding an electron pair is higher. Lepetit et al. performed the ELF analysis of carbo $[N]$ annulenes, including *carbo*-benzene, and reported a double aromaticity for some systems.[51] In Figure 3, the color code employed for ELF is blue for regions

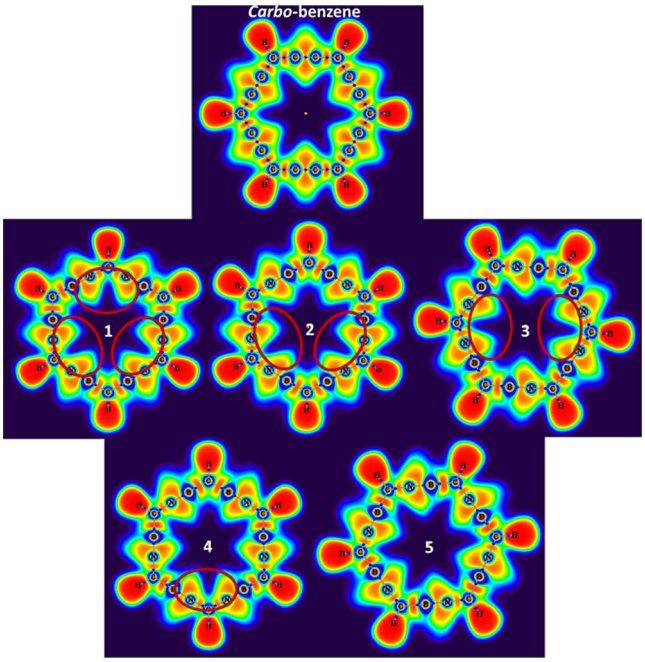

Figure 3. Color-filled map of ELF of the isomers proposed for *iminobora*-benzenes and *carbo*-benzene.

poor in electrons and red for rich-electron regions. For *carbo*-benzene and *iminobora*-benzene, shown in Figure 3, hydrogen atoms are located in red regions, indicating the electron deficiency characteristic of protons. In contrast, boron, carbon, and nitrogen atoms are surrounded by blue regions, signifying the presence of electron density. The ELF map also depicts chemical bonds (C−H, C−B, C−N, and B−N) colored between red and orange. Additionally, the electron pairs around nitrogen atoms appear as orange regions. In these isomers, there is a relationship between energy values and the electron pairs of adjacent nitrogen atoms (indicated by red ellipses in Figure 3). For **1** (the lowest energy isomer), three ellipses are depicted; two ellipses are observed in **2** and **5**, while only one ellipse appears in **4**. Notably, **5** has no ellipses and exhibits the highest relative energy. For comparison, the ELF of *carbo*-benzene is also shown in Figure 3, where no ellipses are observed in the organic ring, similar to what is seen in **5**.

In Figure 4, the isosurfaces of the LOL based solely on π-MOs, labeled as LOL-π,[13,52,53] are depicted. This methodology is a widely used real-space function that reveals the delocalization of π-electron conjugated molecular units. The LOL-π isosurfaces for *carbo*-benzene (above and below the molecular plane) are continuous and homogeneous. For **1** and **5**, the difference in electronegativity between the nitrogen and boron atoms results in discontinuous isosurfaces of their respective LOL-π. These findings are consistent, with the BCP of AIM analysis, as well as the recently reported behavior of benzene, carborazine, and borazine.[53] Additionally, in Figure 4, the LOL-π isosurfaces for **1** and **5**, show that **5** has more homogeneous isosurfaces than those observed in **1**, indicating

https://doi.org/10.1021/acsomega.4c09769
ACS Omega 2025, 10, 5900−5908

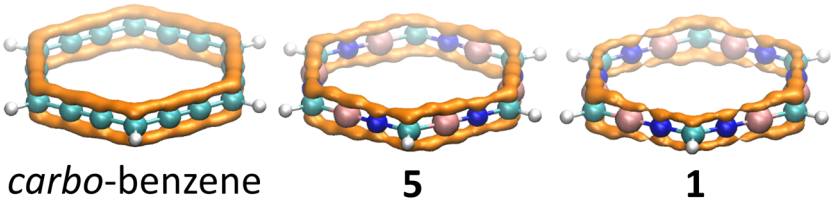

Figure 4. Isosurfaces of LOL-π (isovalue = 0.5) computed on *carbo*-benzene, isomers **5** and **1**.

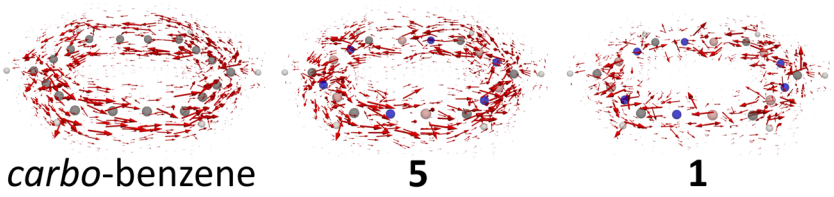

Figure 5. 3D MICD for *carbo*-benzene, isomers **5** and **1**. Counterclockwise represents a diatropic response.

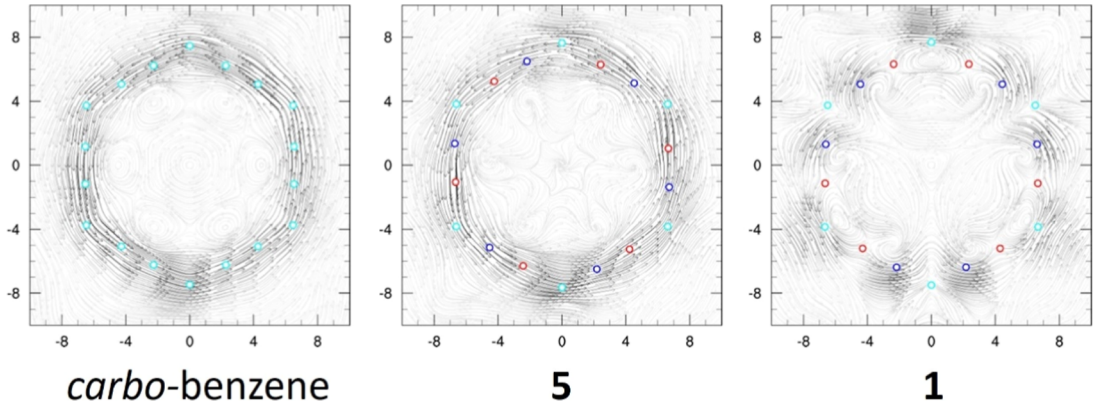

Figure 6. MICD plotted at 2 Bohr over the molecular planes of *carbo*-benzene, **5** and **1**. Hydrogens were omitted for clearness and cyan, red, and blue circles refer to carbon, boron, and nitrogen atoms, respectively. Diatropic (aromatic) response is counterclockwise.

more effective electronic delocalization in **5** (suggesting it is more aromatic).

For the confirmation of the electronic delocalization in the rings, MICD was calculated. 3D plots of the MICD for *carbo*-benzene, as well as for isomers **1** and **5**, are presented in Figure 5. The counterclockwise direction follows the diatropic behavior, which is clearly shown for *carbo*-benzene and **5**, while it is not clear for **1**. The volume slices in the molecular plane, $1a_0$ and $2a_0$ above it, were taken for clearness. Therefore, MICD isolines were plotted for each system, where counterclockwise refers to the diatropic current density. The 3D plots of the MICD for the rest of the isomers, as well as for *iminobora*-borazine, are provided in Figure S15 of the ESI.

None of the systems exhibit a clear diatropic response over the molecular plane; however, if the plane is moved 1 to 2 Bohr above the molecular plane, all systems, except *iminobora*-borazine, exhibit a diatropic current ring. MICD plots for *carbo*-benzene and *iminobora*-borazine, in the molecular plane and at 1 and 2 Bohr, are given in Figure S16 of the ESI. In Figure 6, and the maps of MICD computed for *carbo*-benzene and isomers **1** and **5**, are depicted, clearly illustrating the similarity of **5** to *carbo*-benzene aromatic character. Remarkably, **1** presents the least spatially extended diatropic isolines (see Figure S17 for complete MICD plots of all of the proposed isomers). This diatropic current is associated with an aromatic response when an external magnetic field is applied.

Further analysis of the strength of the current density has been realized. The integral of the MICD was calculated for three different planes. YZ plane, +120, and −120° from the YZ plane, bisecting the triple bond in the original *carbomer*. Results are collected in Table 1 and suggest that the lowest strength current density belongs to *iminobora*-borazine (less than 1.0 nA/T), which is labeled as nonaromatic based on its current density and its strength. This is followed by **1** with an average of 2.5 nA/T, despite its weakness in the current density, it is still present as a clear diatropic response (Figure 6); therefore, it could be considered aromatic. The nonaromatic classification for *iminobora*-borazine as well as the low strength current density over isomer **1** are completely reliable

Table 1. Integration of the Strength of the Current Density in Three Different Planes and Their Respective Mean[a]

system	YZ	+120°	−120°	mean
Carbo−benzene	21.2	29.0	28.9	26.4
Iminobora-benzene	1.10	−1.21	2.40	0.80
1	1.40	5.30	0.90	2.50
2	9.20	19.3	19.3	15.9
3	11.7	22.9	23.2	19.3
4	15.6	21.4	13.8	16.9
5	20.5	19.1	27.9	22.5

[a]All Data in nA/T.

https://doi.org/10.1021/acsomega.4c09769
ACS Omega 2025, 10, 5900−5908

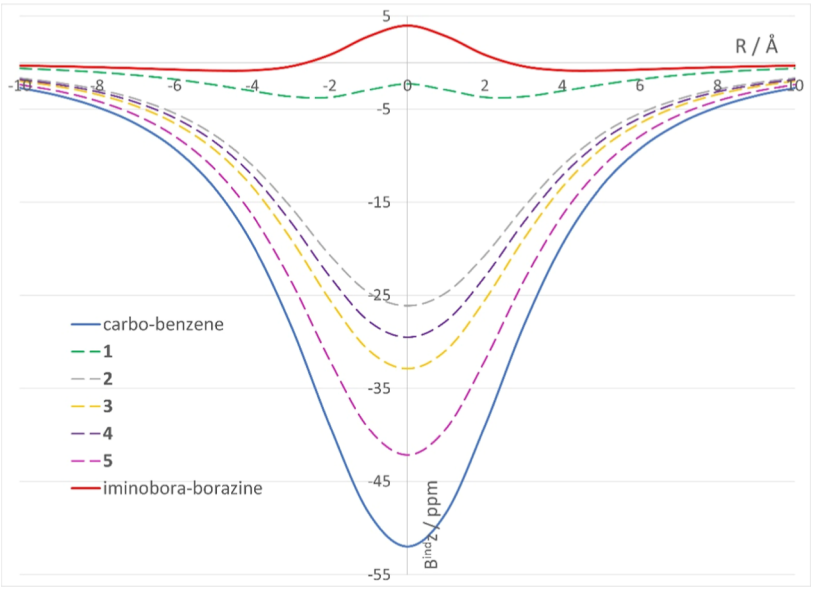

Figure 7. Profiles of the B_z^{ind} computed along the *z*-axis of the *iminobora*-benzene isomers, *carbo*-benzene, and *iminobora*-borazine.

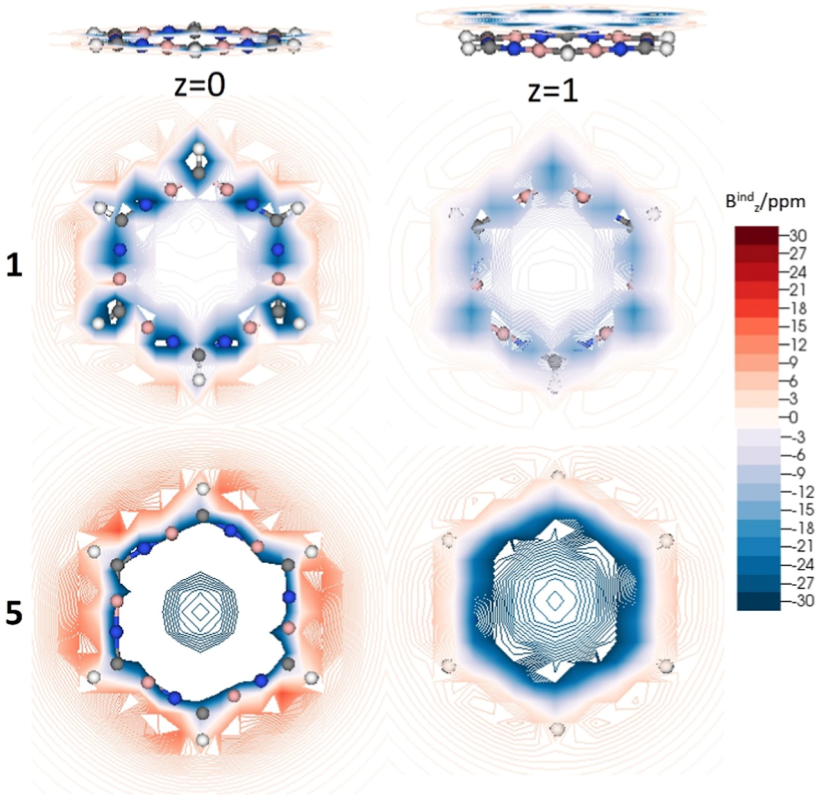

Figure 8. Isolines of the B_z^{ind} computed only in isomers **1** and **5**. Plotted maps are the *xy* planes at $Z = 0$ (molecular plane) and $Z = 1$ (1 Å above the molecular plane). White, gray, blue, and pink spheres represent hydrogen, carbon, nitrogen, and boron atoms, respectively.

in comparison with the B_z^{ind} analysis (*vide infra*). Figure S16 displays the MICD slices of *carbo*-benzene and *iminobora*-borazine at distances of 0, 1, and 2 Bohrs from the molecular plane. A pronounced diatropic response is evident for *carbo*-benzene, whereas it is absent for *iminobora*-borazine. Similarly, Figure S17 presents the MICD slices for all isomers under consideration, revealing a distinct diatropic response at 2 Bohrs from the molecular plane.

For completeness, induced magnetic field calculations were performed. For better reference, the magnetic responses of *carbo*-benzene and *iminobora*-borazine were also computed and reported. With this methodology, **1** can be catalogued as the least diatropic (aromatic) compound; its magnetic response may even be categorized as nonaromatic due to its low diatropic character. Its shape is similar to the profile computed for inorganic *iminobora*-borazine (see Figure 6). In contrast, **5** can be considered the most aromatic isomer, as its diatropic

https://doi.org/10.1021/acsomega.4c09769
ACS Omega 2025, 10, 5900−5908

response is comparable to the magnetic response of the aromatic *carbo*-benzene.

In Figure 7, only the B_z^{ind} isoline maps of the most and the least diatropic isomers (**1** and **5**) are analyzed. Their respective maps show an intense diatropic region generated at the center of compound **5**. Additionally, a homogeneous distribution of the diatropic response is observed along its molecular skeleton. At 1 Å above the molecular plane, the isolines show high diatropic regions distributed over the ring's inner zone and around the positions of the atoms. In contrast, a different situation is observed in isomer **1**, where the diatropic regions are clearly localized around the nitrogen atoms, avoiding the boron atoms. The same response is observed at 1 Å over the ring. The consistency between B_z^{ind} and MICD remains evident across all other isomers. It consistently shows that *carbo*-benzene presents the highest strength and is therefore the most diatropic system (see Figure 8).

Finally, the AV1245 and AVmin electronic aromaticity indices were used to complement the analysis of aromaticity. The AV1245 index quantifies the aromaticity of large rings by averaging the 4c-ESI (4-center electron sharing index) values along the ring of more than six members that maintain a 1, 2, 4, and 5 positional relationships, calculated from the density matrix and the overlap matrix.[39] The AVmin index corresponds to the minimum absolute value of all 4c-ESI values involved in AV1245, quantifying the lowest conjugation pathway of delocalization. A high value of AV1245 and AVmin (AV1245 = 14, for benzene) indicates that the molecule is aromatic, while low values indicate a nonaromatic or antiaromatic character.

Table 2 shows that **5** exhibits the highest degree of electronic delocalization, which is consistent with the analysis of the magnetic field induced in B_z^{ind}, with values comparable to those of *carbo*-benzene. These results indicate that isomer **5** presents a higher aromatic character compared to the rest of the isomers due to the continuous distribution of B and N atoms in the ring, generating a highly delocalized structure. According to the AV1245 index, **3** might show less aromaticity because the distribution of B and N atoms is in opposite positions on all sides of the ring. However, **4** probably has the least aromatic character according to the AVmin index, since one of the vertices forms BCB bonds, while the opposite vertex forms NCN bonds. This result does not agree with B_z^{ind}, which indicates that **1** is the least aromatic. Although these indices of aromaticity agree in predicting the molecule with the highest aromatic character, the noncontinuous distribution of the B and N atoms of the BN units in the ring influences the electronic delocalization in **1**, **2**, **3**, and **4**.

Table 2. Values of Different Methodologies Employed for the Study of Aromaticity

molecule	B_z^{ind} (1)/ppm	AV1245	AVmin
1	−2.9	3.26	0.67
2	−24.7	3.50	0.60
3	−30.9	3.19	0.70
4	−27.8	4.52	0.25
5	−39.3	5.36	2.79
carbo-benzene	−48.4	5.58	5.33
iminobora-borazine	2.8	1.43	0.30

This apparent discrepancy between magnetic indices (MICD−B_z^{ind}) and electronic indices (AV1245) could be explained by their nature. It is important to recall that magnetic indices are sensitive to the measuring position, e.g., incorporating diatropic local responses into the total response. Therefore, the aromatic response in this set shifts the ordering between compounds **3** and **4**. As observed in Figure S17, isomer **4** exhibits more diatropic local regions than **3**, increasing its total diatropic response. While magnetic indices show slight variations: 3 ppm for B_z^{ind} and 2.4 nAT^{-1} for MICD. They correlate well with other aromatic rankings. On the other hand, AV1245 shows an apparent and subtle discrepancy with other aromatic indices, yet it perfectly agrees with the position of RCP (Table S1). Thus, AV1245 values are a result of how the electrons are shared among multiple centers. It makes it inherently related to the electron density distribution and the critical points of a system. This highlights the importance of analyzing aromaticity from different vertices such as electronic, geometric, magnetic, and energetic. As demonstrated in this work, each one provided unique insights and, at times, they reveal discrepancies or counterintuitive results among the different indices or even in the same index.

4. CONCLUSIONS

The orientation of the BN units has an impact on the electronic delocalization of the *iminobora*-benzenes but does not affect their structural parameters, such as planarity and bond lengths. Also, the relative energy of the isomers is strongly dependent on the orientation of the B and N atoms. With AdNDP, MICD, B_z^{ind}, AV1245, and AVmin, **5** was identified as the most aromatic isomer. Interestingly, this isomer is also the least stable in terms of the relative energy. Some possible explanations could be attributed to the high relative energy of **5**, e.g., to the presence of six carbon atoms with negative charges. In contrast, **1** is the most stable isomer in terms of relative energy; however, some of the indices (MICD, B_z^{ind}) used in this study classify it as nearly nonaromatic. This counterintuitive situation has also been recently published by Cheng et al.[8] It cannot be attributed to either structural stress or any other topological parameter except the ESP over the isomers, which shows a positive correlation with the relative energy. These results may provide insights into the importance of the orientation of highly polarized chemical entities such as BN units in molecules with electronic delocalization. Besides, it potentially could tune some properties, based on its aromatic character. It is known that borazine prefers addition reactions over substation reactions. Fine tuning the aromaticity in these extended rings could provide specific reaction pathways or even different reactions, such as electrophilic reactions;[18,19] or even more, paving the way to new stable sandwich-like system for catalysis.

■ ASSOCIATED CONTENT

Supporting Information

The Supporting Information is available free of charge at https://pubs.acs.org/doi/10.1021/acsomega.4c09769.

Topological parameters of the RCPs, complete set plots of molecular orbitals, AdNDP isosurfaces, ring currents maps and Cartesian coordinates of the isomers, and *carbo*-benzene and *iminobora*-borazine (PDF)

https://doi.org/10.1021/acsomega.4c09769
ACS Omega 2025, 10, 5900−5908

AUTHOR INFORMATION

Corresponding Authors

Luz Diego − *Doctorado en Fisicoquímica Molecular, Facultad de Ciencias Exactas, Universidad Andres Bello, Santiago 8370146, Chile*; Email: l.diegoramon@uandresbello.edu

Rafael Islas − *Departamento de Ciencias Químicas, Facultad de Ciencias Exactas and Centro de Química Teórica & Computacional (CQT&C), Facultad de Ciencias Exactas, Universidad Andres Bello, Santiago 8370146, Chile*; orcid.org/0000-0001-5655-107X; Email: rafael.islas@unab.cl

Authors

David Arias-Olivares − *Center of Applied Nanoscience (CANS), Facultad de Ciencias Exactas, Universidad Andres Bello, Santiago 8370146, Chile*; orcid.org/0000-0002-1701-8288

Diego V. Moreno − *Laboratorio de Química Computacional, Programa de Química, Universidad de Ciencias Aplicadas y Ambientales (U.D.C.A.), Bogotá 111166, Colombia*

Erick Cerpa − *Departamento de Formación Básica y Disciplinaria, Unidad Profesional Interdisciplinaria de Ingeniería Campus Guanajuato, Instituto Politécnico Nacional, Silao de La Victoria Gto C.P. 36275, Mexico*; orcid.org/0009-0005-3610-6573

Complete contact information is available at: https://pubs.acs.org/10.1021/acsomega.4c09769

Notes

The authors declare no competing financial interest.

ACKNOWLEDGMENTS

L.D. acknowledges the National Agency for Research and Development (ANID)/Scholarship Program/becas doctorado nacional/2023-21231670 (L.D.).

REFERENCES

(1) Chauvin, R.; Carbomers, I. A general concept of expanded molecules. *Tetrahedron Lett.* **1995**, *36* (3), 397−400.

(2) Chauvin, R. Carbomers". II. En route to [C,C]6carbo-benzene. *Tetrahedron Lett.* **1995**, *36* (3), 401−404.

(3) Maraval, V.; Chauvin, R. From Macrocyclic Oligo-acetylenes to Aromatic Ring *Carbo*-mers. *Chem. Rev.* **2006**, *106* (12), 5317−5343.

(4) Jalife, S.; Audiffred, M.; Islas, R.; Escalante, S.; Pan, S.; Chattaraj, P. K.; Merino, G. The inorganic analogues of carbo-benzene. *Chem. Phys. Lett.* **2014**, *610*−*611*, 209−212.

(5) Cocq, K.; Lepetit, C.; Maraval, V.; Chauvin, R. *Carbo*-aromaticity" and novel *carbo*-aromatic compounds. *Chem. Soc. Rev.* **2015**, *44* (18), 6535−6559.

(6) Azpiroz, J. M.; Islas, R.; Moreno, D.; Fernández-Herrera, M. A.; Pan, S.; Chattaraj, P. K.; Martínez-Guajardo, G.; Ugalde, J. M.; Merino, G. *Carbo*-Cages: A Computational Study. *J. Org. Chem.* **2014**, *79* (12), 5463−5470.

(7) Arias-Olivares, D.; Becerra-Buitrago, A.; García-Sánchez, L. C.; Moreno, D. V.; Islas, R. In Silico Analysis of the Aromaticity of Some *Carbo*-Metallabenzenes and *Carbo*-Dimetallabenzenes (*Carbo*-mers Proposed from Metallabenzenes). *ACS Omega* **2024**, *9* (9), 10913−10928.

(8) Cheng, X.; Sun, C.; Cheng, X. Aromaticity and substitution effect of the mono-boron-nitrogen-replaced analogues of cyclo[18]-carbon. *Chem. Phys. Lett.* **2025**, *860*, 141816.

(9) Baranac-Stojanović, M. Aromaticity and Stability of Azaborines. *Chem. - Eur. J.* **2014**, *20* (50), 16558−16565.

(10) Srivastava, A. K.; Misra, N. Introducing "carborazine" as a novel heterocyclic aromatic species. *New J. Chem.* **2015**, *39* (4), 2483−2488.

(11) Anstöter, C. S.; Gibson, C. M.; Fowler, P. W. Modelling aromatisation of $(BN)_nH_{2n}$ azabora-annulenes. *Phys. Chem. Chem. Phys.* **2020**, *22* (28), 15919−15925.

(12) Kalemos, A. The nature of the chemical bond in borazine ($B_3N_3H_6$), boroxine ($B_3O_3H_3$), carborazine ($B_2N_2C_2H_6$), and related species. *Int. J. Quantum Chem.* **2018**, *118* (16), No. e25650.

(13) Wu, Y.; Liu, Z.; Lu, T.; Orozco-Ic, M.; Xu, J.; Yan, X.; Wang, J.; Wang, X. Exploring the aromaticity differences of isoelectronic species of cyclo [18] carbon (C_{18}), $B_6C_6N_6$, and B_9N_9: The role of carbon atoms as connecting bridges. *Inorg. Chem.* **2023**, *62* (49), 19986−19996.

(14) Fowler, P. W.; Mizoguchi, N.; Bean, D. E.; Havenith, R. W. A. Double Aromaticity and Ring Currents in All-Carbon Rings. *Chem. - Eur. J.* **2009**, *15* (28), 6964−6972.

(15) Chandrasekhar, J.; Jemmis, E. D.; von Ragué Schleyer, P. Double aromaticity: aromaticity in orthogonal planes. The 3,5-dehydrophenyl cation. *Tetrahedron Lett.* **1979**, *20* (39), 3707−3710.

(16) Stock, A.; Pohland, E.; Borwasserstoffe, I. X. $B_3N_3H_6$. *Ber. Dtsch. Chem. Ges.* **1926**, *59* (9), 2215−2223.

(17) Wiberg, E. Das "anorganische Benzol" $B_3N_3H_6$ und seine Methylhomologen. *Naturwissenschaften* **1948**, *35* (7), 212−218.

(18) Chiavarino, B.; Crestoni, M. E.; Fornarini, S. Electrophilic Substitution of Gaseous Borazine. *J. Am. Chem. Soc.* **1999**, *121* (11), 2619−2620.

(19) Chiavarino, B.; Crestoni, M. E.; Marzio, A. D.; Fornarini, S.; Rosi, M. Gas-Phase Ion Chemistry of Borazine, an Inorganic Analogue of Benzene. *J. Am. Chem. Soc.* **1999**, *121* (48), 11204−11210.

(20) Islas, R.; Chamorro, E.; Robles, J.; Heine, T.; Santos, J. C.; Merino, G. Borazine: to be or not to be aromatic. *Struct. Chem.* **2007**, *18* (6), 833−839.

(21) Hoffmann, R. Building Bridges Between Inorganic and Organic Chemistry (Nobel Lecture). *Angew. Chem., Int. Ed.* **1982**, *21* (10), 711−724.

(22) Islas, R.; Arias-Olivares, D.; Becerra-Buitrago, A.; García-Sánchez, L. C.; Méndez-Ayón, L. N.; Zuniga-Gutierrez, B. Metallaborazines: To Be or Not To Be Delocalized. *ACS Omega* **2021**, *6* (30), 19629−19641.

(23) Timoshkin, A. Y.; Frenking, G. True" Inorganic Heterocycles: Structures and Stability of Group 13−15 Analogues of Benzene and Their Dimers. *Inorg. Chem.* **2003**, *42* (1), 60−69.

(24) Merino-García, M. d. R.; Soriano-Agueda, L. A.; Guzmán-Hernández, J. d. D.; Martínez-Otero, D.; Landeros Rivera, B.; Cortés-Guzmán, F.; Barquera-Lozada, J. E.; Jancik, V. Benzene and Borazine, so Different, yet so Similar: Insight from Experimental Charge Density Analysis. *Inorg. Chem.* **2022**, *61* (18), 6785−6798.

(25) Perdew, J. P.; Burke, K.; Ernzerhof, M. Generalized Gradient Approximation Made Simple. *Phys. Rev. Lett.* **1996**, *77* (18), 3865−3868.

(26) Perdew, J. P.; Burke, K.; Ernzerhof, M. Generalized Gradient Approximation Made Simple. *Phys. Rev. Lett.* **1997**, *78* (7), 1396.

(27) Adamo, C.; Barone, V. Toward reliable density functional methods without adjustable parameters: The PBE0 model. *J. Chem. Phys.* **1999**, *110* (13), 6158−6170.

(28) Weigend, F.; Ahlrichs, R. Balanced basis sets of split valence, triple zeta valence and quadruple zeta valence quality for H to Rn: Design and assessment of accuracy. *Phys. Chem. Chem. Phys.* **2005**, *7* (18), 3297−3305.

(29) Frisch, M. J.; Trucks, G. W.; Schlegel, H. B.; Scuseria, G. E.; Robb, M. A.; Cheeseman, J. R.; Scalmani, G.; Barone, V.; Petersson, G. A.; Nakatsuji, H.; Li, X.; Caricato, M.; Marenich, A. V.; Bloino, J.; Janesko, B. G.; Gomperts, R.; Mennucci, B.; Hratchian, H. P.; Ortiz, J. V.; Izmaylov, A. F.; Sonnenberg, J. L.; Williams; Ding, F.; Lipparini, F.; Egidi, F.; Goings, J.; Peng, B.; Petrone, A.; Henderson, T.; Ranasinghe, D.; Zakrzewski, V. G.; Gao, J.; Rega, N.; Zheng, G.; Liang, W.; Hada, M.; Ehara, M.; Toyota, K.; Fukuda, R.; Hasegawa, J.; Ishida, M.; Nakajima, T.; Honda, Y.; Kitao, O.; Nakai, H.; Vreven, T.; Throssell, K.; Montgomery, J. A.; Peralta, J. E.; Ogliaro, F.; Bearpark, M. J.; Heyd, J. J.; Brothers, E. N.; Kudin, K. N.; Staroverov, V. N.;

https://doi.org/10.1021/acsomega.4c09769
ACS Omega 2025, 10, 5900−5908

Keith, T. A.; Kobayashi, R.; Normand, J.; Raghavachari, K.; Rendell, A. P.; Burant, J. C.; Iyengar, S. S.; Tomasi, J.; Cossi, M.; Millam, J. M.; Klene, M.; Adamo, C.; Cammi, R.; Ochterski, J. W.; Martin, R. L.; Morokuma, K.; Farkas, O.; Foresman, J. B.; Fox, D. J. *Gaussian 16 Rev. B.01*: Wallingford, CT, 2016.
(30) Seeger, R.; Pople, J. A. Self-consistent molecular orbital methods. XVIII. Constraints and stability in Hartree−Fock theory. *J. Chem. Phys.* **1977**, *66* (7), 3045−3050.
(31) Bauernschmitt, R.; Ahlrichs, R. Stability analysis for solutions of the closed shell Kohn−Sham equation. *J. Chem. Phys.* **1996**, *104* (22), 9047−9052.
(32) Keith, T. A. *AIMAll (Version 19.10.12)*; Gristmill Software: Overland Park KS: USA, 2019.
(33) Reed, A. E.; Weinstock, R. B.; Weinhold, F. Natural population analysis. *J. Chem. Phys.* **1985**, *83* (2), 735−746.
(34) Glendening, E. D.; Landis, C. R.; Weinhold, F. Erratum: NBO 6.0: Natural bond orbital analysis program. *J. Comput. Chem.* **2013**, *34* (24), 2134.
(35) Zubarev, D. Y.; Boldyrev, A. I. Developing paradigms of chemical bonding: adaptive natural density partitioning. *Phys. Chem. Chem. Phys.* **2008**, *10* (34), 5207−5217.
(36) Zubarev, D. Y.; Boldyrev, A. I. Revealing Intuitively Assessable Chemical Bonding Patterns in Organic Aromatic Molecules via Adaptive Natural Density Partitioning. *J. Org. Chem.* **2008**, *73* (23), 9251−9258.
(37) Lu, T.; Chen, F. Multiwfn: A multifunctional wavefunction analyzer. *J. Comput. Chem.* **2012**, *33* (5), 580−592.
(38) Humphrey, W.; Dalke, A.; Schulten, K. V. M. D. VMD: Visual molecular dynamics. *J. Mol. Graph.* **1996**, *14* (1), 33−38.
(39) Matito, E. An electronic aromaticity index for large rings. *Phys. Chem. Chem. Phys.* **2016**, *18* (17), 11839−11846.
(40) Casademont-Reig, I.; Woller, T.; Contreras-García, J.; Alonso, M.; Torrent-Sucarrat, M.; Matito, E. New electron delocalization tools to describe the aromaticity in porphyrinoids. *Phys. Chem. Chem. Phys.* **2018**, *20* (4), 2787−2796.
(41) Saue, T.; Jensen, H. A. Linear response at the 4-component relativistic level: Application to the frequency-dependent dipole polarizabilities of the coinage metal dimers. *J. Chem. Phys.* **2003**, *118* (2), 522−536.
(42) *for PyNGL, developed at the National Center for Atmospheric Research*. 2019.
(43) Saue, T.; Bast, R.; Gomes, A. S. P.; Jensen, H. J. A.; Visscher, L.; Aucar, I. A.; Di Remigio, R.; Dyall, K. G.; Eliav, E.; Fasshauer, E.; Fleig, T.; Halbert, L.; Hedegård, E. D.; Helmich-Paris, B.; Iliaš, M.; Jacob, C. R.; Knecht, S.; Laerdahl, J. K.; Vidal, M. L.; Nayak, M. K.; Olejniczak, M.; Olsen, J. M. H.; Pernpointner, M.; Senjean, B.; Shee, A.; Sunaga, A.; van Stralen, J. N. P. The DIRAC code for relativistic molecular calculations. *J. Chem. Phys.* **2020**, *152* (20), 204104.
(44) Dunning, Jr. T. H. Gaussian basis sets for use in correlated molecular calculations. I. The atoms boron through neon and hydrogen. *J. Chem. Phys.* **1989**, *90* (2), 1007−1023.
(45) Islas, R.; Heine, T.; Merino, G. The Induced Magnetic Field. *Acc. Chem. Res.* **2012**, *45* (2), 215−228.
(46) Schleyer, P. v. R.; Maerker, C.; Dransfeld, A.; Jiao, H. J.; van Eikema Hommes, N. J. R. Nucleus-independent chemical shifts: A simple and efficient aromaticity probe. *J. Am. Chem. Soc.* **1996**, *118* (26), 6317−6318.
(47) Soncini, A.; Fowler, P. W.; Černušak, I.; Steiner, E. C. 6h-Hexa-azahexaborine, [(CH)BN]6: structure and magnetic properties of a proposed 18-electron aromatic ring. *Phys. Chem. Chem. Phys.* **2001**, *3* (18), 3920−3923.
(48) Becke, A. D.; Edgecombe, K. E. A simple measure of electron localization in atomic and molecular systems. *J. Chem. Phys.* **1990**, *92* (9), 5397−5403.
(49) Silvi, B.; Savin, A. Classification of chemical bonds based on topological analysis of electron localization functions. *Nature* **1994**, *371* (6499), 683−686.
(50) Jacobsen, H. Localized-orbital locator (LOL) profiles of chemical bonding. *Can. J. Chem.* **2008**, *86* (7), 695−702.
(51) Lepetit, C.; Silvi, B.; Chauvin, R. ELF Analysis of Out-of-Plane Aromaticity and In-Plane Homoaromaticity in Carbo[N]annulenes and [N]Pericyclynes. *J. Phys. Chem. A* **2003**, *107* (4), 464−473.
(52) Lu, T.; Chen, Q. A simple method of identifying π orbitals for non-planar systems and a protocol of studying π electronic structure. *Theor. Chem. Acc.* **2020**, *139* (2), 25.
(53) Wu, Y.; Yan, X.; Liu, Z.; Lu, T.; Zhao, M.; Xu, J.; Wang, J. Aromaticity in Isoelectronic Analogues of Benzene, Carborazine and Borazine, from Electronic Structure and Magnetic Property. *Chem. - Eur. J.* **2024**, *30* (66), No. e202403369.

https://doi.org/10.1021/acsomega.4c09769
ACS Omega 2025, 10, 5900−5908